135 PRELIMINARY ASSESSMENT OF TIMING DIFFERENCES BETWEEN CONVECTIVE INITIATION AND SEVERE INITIATION

Stuart D. Miller, Jr.*[,2,4] and James Correia[1,3]

[1]NOAA/NWS/NCEP/Storm Prediction Center, Norman, Oklahoma

[2]USAF Institute of Technology Civilian Institution Programs, Wright-Patterson AFB, OH

[3]Cooperative Institute for Mesoscale Meteorological Studies, Norman, OK

[4]University of Oklahoma School of Meteorology, Norman, OK

1. INTRODUCTION

Little has been done to systematically evaluate time between convective initiation (CI) and when that convection meets severe criteria (hereafter known as severe initiation, or SI). Bluestein and Parker (1993, Table 2) found that for a sample of 36 storms of varying convective mode, the average time between CI and tornado touchdown was 2.18 h, with a standard deviation of 0.98 h. In that study, CI was defined as the appearance of first radar echo at "low elevation angle."

Bluestein (2009) detailed the initiation and evolution of the supercell that produced the Greensburg, KS tornado on 4 May 2007. Here, CI was defined as the presence of first precipitation radar echoes, and it was discovered that the storm that would eventually strike Greensburg first became tornadic approximately 1 h after meeting this criterion. Ziegler et al. (2001) examined the storm complex that affected Newcastle and Graham, TX on 29 May 1994. While the actual time of CI was given rather ambiguously (as this was not the focus of the study), it appears that tornado touchdown in this storm occurred between 1.5 and 2 h after CI.

The motivation for this work is to inform forecasters on the timing difference between CI and SI. The hope is that it will aid in decision-making of when to issue convective watches, or when to anticipate severe storm warnings, given they know the approximate predicted time of CI. To begin to meet that need, this investigation will focus exclusively on systematically and objectively defining the time between CI and SI. The aforementioned papers used rather ambiguous criteria for CI, such as "appearance of first radar echo." It is unclear what this means in terms of radar elevation angle, dBZ threshold, and longevity of that echo. A precise definition of CI used in this study will be given in Section 2.

Section 2 gives the methodology of this work, Section 3 summarizes the results, Section 4 offers some preliminary conclusions from those results, Section 5 contains references, and Section 6 presents all relevant figures.

2. METHODOLOGY

A definition for CI based on that which is currently being implemented in the NOAA Hazardous Weather Testbed for the Spring Forecasting Experiment will be used for this investigation. That definition requires a convectively active object to contain at least 35 dBZ at the -10ºC level (MTR35), and maintain this criterion for at least 30 min (Kain et al. 2012). If these criteria are met, only the earliest instance of the object is labeled as CI. For the purposes of this paper, it will be modified to require convective objects to contain at least four continuous MTR35 grid points and at least one grid point of 40 dBZ at the -10ºC level. The first observation time that a convective object meets these criteria is considered the time of CI. There is no longevity component to the convective object definition used in this study.

Observed reflectivity at -10ºC originally on the National Mosaic & Multi-Sensor QPE (NMQ) (Zhang et al. 2011) grid was used to determine convective objects. The -10ºC level was computed using the Rapid Update Cycle (RUC) model. The reflectivity data were thinned to a temporal resolution of 15 min and then

* *Corresponding author address:* Stuart Miller, 120 David L. Boren Blvd, Suite 2200, Norman, OK, 73072
E-mail: stuart.miller@ou.edu

interpolated via a budget scheme to the Center for Analysis and Prediction of Storms (CAPS) model grid. The CAPS grid has a horizontal grid spacing of 4 km, and includes approximately the eastern two-thirds of the United States (measuring 863 grid points in the x-direction by 693 grid points in the y-direction).

To make an uncontaminated assessment of CI timing, it was important to choose cases and experimental domains that started out as "clean-slate" as possible. These domains lacked ongoing convection or pre-existing storm-scale boundaries so convection that developed in them was forced by meso- to synoptic-scale processes. This allowed for the best evaluation of true CI timing. In all, 15 cases from May-June 2011 (during the period of the 2011 Spring Forecasting Experiment) were found (Fig. 1).

Due to the criteria chosen for defining convective objects, the overall number of objects in the domain as time progressed became insignificant. At the -10ºC level, it can be generally difficult to discern discrete storms using a reflectivity threshold as low as 35 dBZ, especially when they mature and/or occur in close proximity to each other. Therefore, in cases where convection grew upscale, individual convective cores within the system often could not be resolved, and the number of storms tended to decrease with time. The goal of this work, however, was to capture CI at its earliest stages to make the best assessment of time difference between CI and SI, hence the reason such relaxed dBZ constraints were implemented.

In order to compare CI timing to SI timing, local storm reports (LSR's) from the Storm Data database was used. Admittedly, this database contains drawbacks (Trapp et al., 2006), due to errors in timing and location of some reports. Once it is quality-controlled by the Storm Prediction Center, however, many erroneous and duplicate reports are excluded. This makes Storm Data the most useful database of its kind for collecting statistics for the purposes of this paper.

Convective objects meeting the aforementioned criteria were defined and tracked within these domains, and the domains were searched for LSR's. If a report occurred in the domain within the last 15 min of each observation time, it was associated with the convective objects in the domain at that time. That is to say, since the domains were designed to surround each specific CI event, the reports were not being associated with specific objects, but the event itself. Time series spanning 1300 UTC to 0000 UTC the next day were created for the sixteen cases, at 15-min resolution, so the timing difference between CI and SI associated with each CI event could be determined. Also analyzed were timing trends of total LSR's as well as each report type relative to CI.

A complicating factor occurred when a second round of convection lagged the CI event being evaluated. If this later convection entered the verification domain, severe reports associated with it would pollute the results, since the domain was searched for objects and reports every 15 min. To prevent this problem, some of the domains had to be "advected" with the CI event so that transient storms that were not associated with the CI did not enter their boundaries.

3. RESULTS

Fig. 2 depicts the convective object/severe report time series for two examples from the 15 cases examined. Fig. 2a is from 19 May, 2011, and Fig. 2c is a corresponding radar image from that day valid at 1915 UTC. From Fig. 2a, convective objects are detected at 1745 UTC (time of CI). SI is at 1800 UTC with the first severe reports being hail. At the time of the still image (1915 UTC) in Fig. 2c, there are four distinct convective objects that are contoured and three hail reports which correspond to the time series in Fig. 2a. Figs. 2b and 2d are interpreted in the same way as Figs. 2a and 2c, except they are valid for a separate case on 25 May, 2011.

The aggregates of all cases are given in Figs. 3-6. Fig. 3 shows the frequency of SI (first report) for each case by report type (hail, tornado, wind) as a function of difference from CI time. It is evident that a majority of SI occurred within the first two hours after CI. Additionally, the largest number of first reports happened 0.5 h after CI, and the most frequent SI report type was hail (66.7%). This was followed by wind (33.3%), and none of the SI reports were tornado. The average amount of time between CI and SI was 1.15 h and 1.05 h with standard deviations of 1.25 h and 0.60 h for hail and wind, respectively. The outlier hail report at 4.50 h after CI greatly affected the average and standard deviation of timing difference from CI for hail. This was a case of isolated CI during the late morning on 1 June 2011 over North-Central Kansas. It became multicellular in nature and took several hours to organize and develop a substantial reflectivity core. Neglecting this outlier gives hail occurrence an average of 0.78 h, and a standard deviation of 0.44 h, after CI.

Fig. 4 is the Probability Distribution Function (PDF) of Fig. 3. Given that a storm undergoes SI, SI is most likely to occur 0.5 h after CI. Hail was the most probable during this time.

Fig. 5 is similar to Fig. 3, except that it depicts the difference in timing from CI for all severe reports associated with the CI events in the sample. It appears that a majority of the reports occurred between 1.25 and 3.0 h after CI. Hail was the most common report ahead of wind and then tornado. The average time after CI for all reports was 2.50 h, 2.52 h, and 3.39 h with standard deviations of 1.30 h, 1.24 h, and 1.77 h for hail, tornadoes, and wind, respectively. Severe reports never occurred earlier than 0.25 h, and rarely occurred earlier than 0.5 h, after CI. Initial severe threats were from hail and wind, and tornadoes became more likely as time progressed.

It bears noting that the distributions of hail and tornado reports appear very similar to one another. Upon examination of Fig. 6, which is the PDF of Fig. 5, each appears to follow a gamma-like PDF. Wind reports, however, are more evenly distributed between 0 and 7 hours after CI. They are even a bit skewed toward the later stages of storms' lifetimes, i.e. past 3.5 hours.

4. CONCLUSION

In environments conducive to tornadic storms, the earliest threats were from hail and wind. This certainly should not come as a surprise as it is what is generally observed, but it is worth emphasizing that these data support that notion.

Most SI occurred within the first 2 h after CI. A majority of the SI report types were hail occurring 0.5 h after CI. Since the SI dataset (Figs. 2 and 3) only included 15 data points (there was one SI time per case), it would be more robust to draw general conclusions from all reports in the dataset (Figs. 4 and 5, 285 data points). Given that reports occurred, they were most probable to occur between 1.50 to 2.75 h after CI. From a watch- and warning-decision standpoint, the data for all reports suggest that the forecaster has approximately 1.25 to 3.75 h between CI and SI (taking into account the average and standard deviations between CI and all severe development and interpolating to the temporal resolution of the dataset). It could be inferred that the more favorable the environment for severe storms, the earlier SI should occur. This is due to the fact that in these environments, individual storms would not have to rely as heavily on internal dynamics to become severe because necessary ingredients would be supplied by the ambient environment. Future work comparing SI time to convective parameters would be necessary to confirm this hypothesis. If the forecaster desires an hour of lead time on a watch, for example, they can conceivably wait until signs of CI are observed (or possibly later, depending on conditions) to issue that watch.

As stated in the introduction, the primary goal of this study is to provide forecasters with information to help them decide when they can expect storms to become severe after initiation. Even though the sample used here was relatively small, some important, albeit preliminary, trends can be discerned to aid forecasters in better predicting when SI will occur. This could allow for more confident watch issuance times and better anticipation of when warnings might be necessary.

5. REFERENCES

Bluestein, H.B. and S.S. Parker, 1993: Modes of isolated, severe convective storm formation along the dryline. *Mon. Wea. Rev.,* **121,** 1354-1372.

Bluestein, H.B., 2009: The formation and early evolution of the Greensburg, Kansas, tornadic supercell on 4 May 2007. *Wea. Forecasting,* **24,** 899-920.

Kain, J.S., M.C. Coniglio, J. Correia, A.J. Clark, P.T. Marsh, C.L. Ziegler, V. Lakshmanan, S.D. Miller, S.R. Dembek, S.J. Weiss, F. Kong, M. Xue, R.A. Sobash, A.R. Dean, I.L. Jirak, C.J. Melick, 2012: A feasibility study for probabilistic convection initiation forecasts based on explicit numerical guidance. Conditionally accepted for publication in the *Bull. Amer. Meteor. Soc.*

Trapp, R.J., D.M. Wheatley, N.T. Atkins, R.W. Przybylinski, and R. Wolf, 2006: Buyer beware: Some words of caution on the use of severe wind reports in postevent assessment and research. *Wea. Forecasting,* **21,** 408-415.

Zhang, J., and Coauthors, 2011: National mosaic and multi-sensor QPE (NMQ) system: description, results, and future plans. Bull. Amer. Meteor. Soc., **92**, 1321–1338.

Ziegler, C.L., E.N. Rasmussen, T.R. Shepherd, A.I. Watson, and J.M. Straka, 2001: The evolution of low-level rotation in the 29 May 1994 Newcastle-Graham, Texas, storm

complex during VORTEX. *Mon. Wea. Rev.,* **129,** 1339-1368.

6. FIGURES

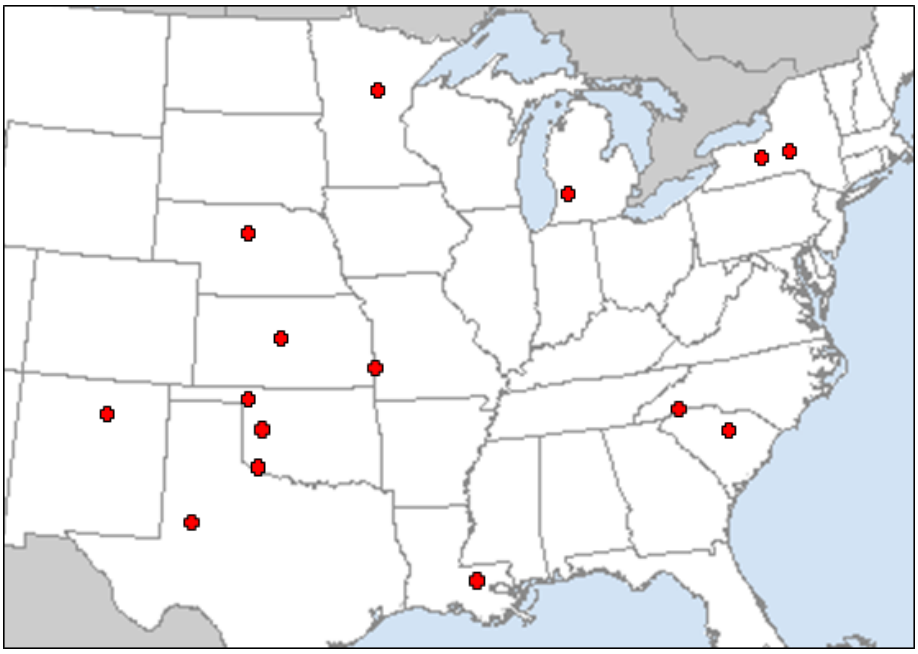

FIG. 1. Locations of the 15 clean-slate CI events evaluated.

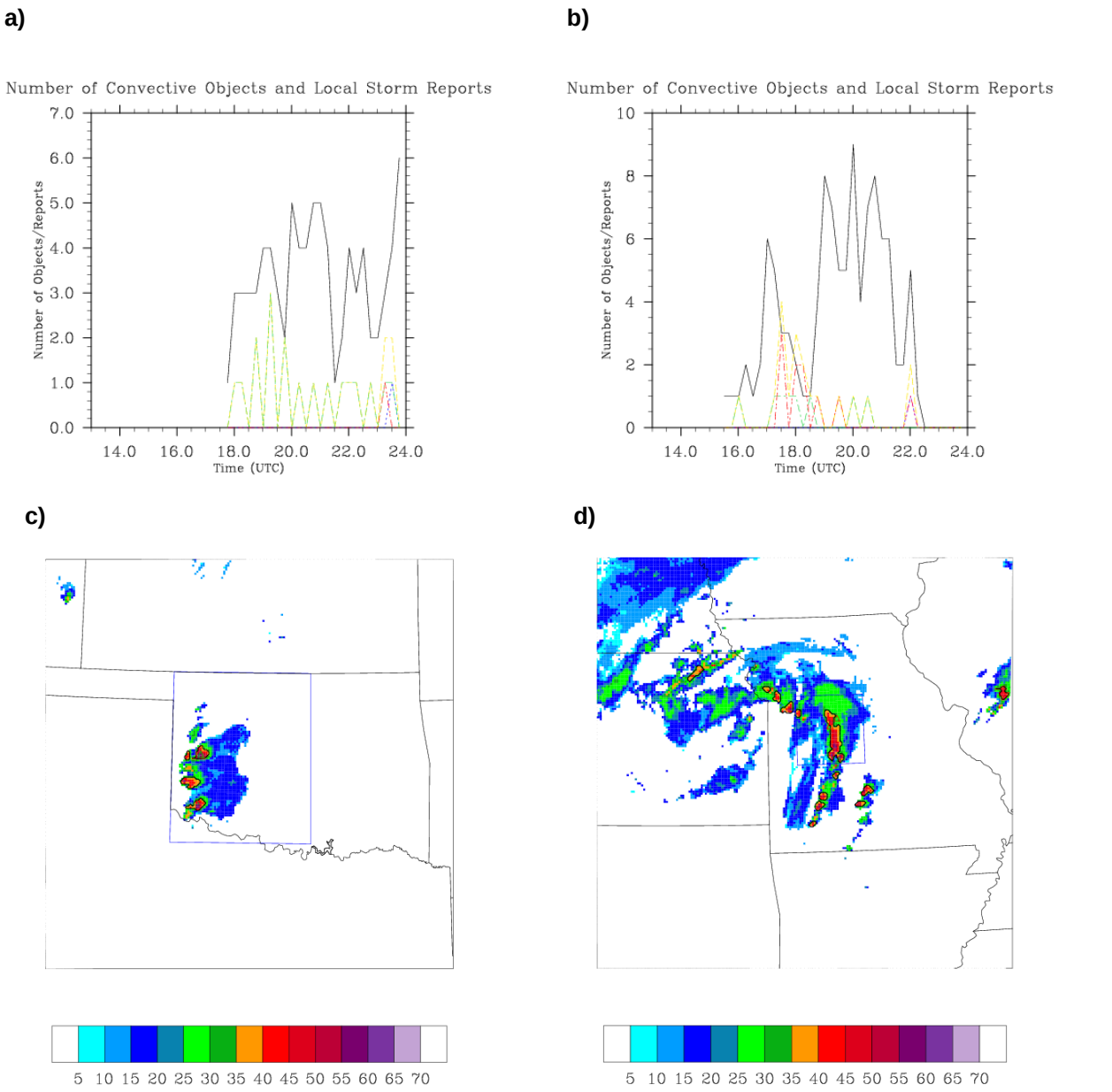

FIG. 2. Top: Example time series of convective objects and severe reports associated with those objects in the domain for two of the 15 cases examined. Convective objects are in black, total LSR's in yellow, hail reports in green, wind reports in blue, and tornado reports in red. Time series are valid for a) 19 May 2011 over Oklahoma, and b) 25 May 2011 over Missouri. Bottom: Sample observation times corresponding to the dates of the time series above them. c) is valid at 1915 UTC on 19 May 2011 and d) is valid at 1730 UTC on 25 May 2011. The domain is depicted by the blue box, convective objects are contoured in black, reflectivity is color-filled, and LSR's are indicated by triangles (green-hail, blue-wind, red-tornado). Only convective objects and LSR's inside the domain were considered in this study.

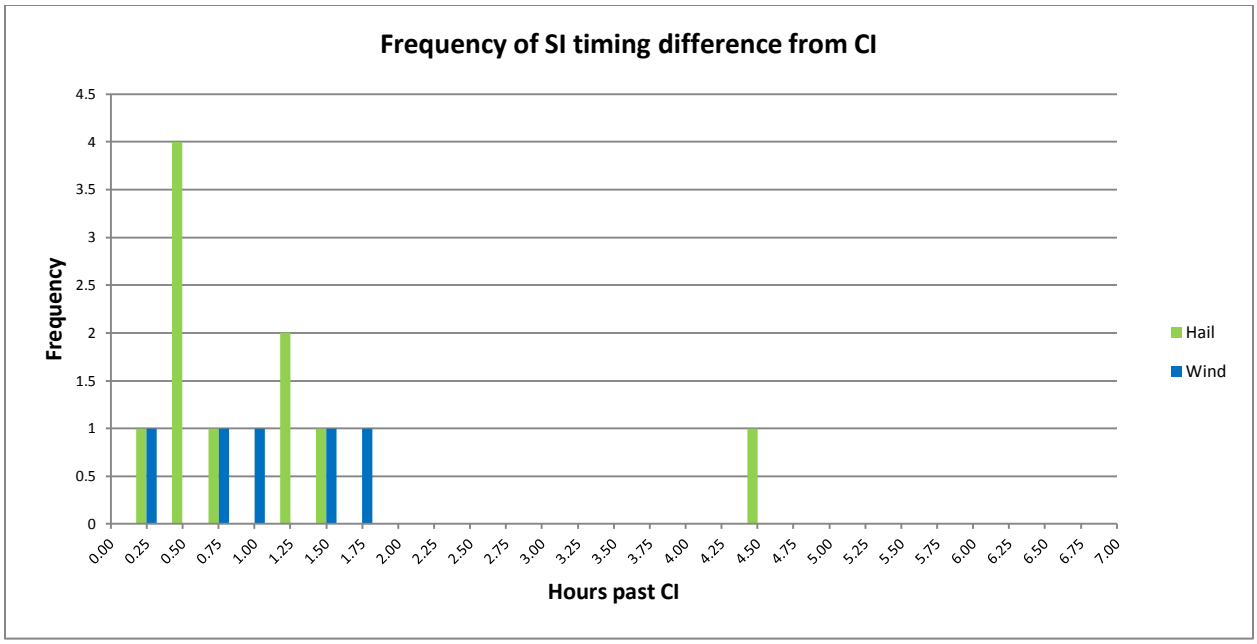

FIG. 3. Histogram depicting the time between observed CI and SI associated with convection for each case in the sample.

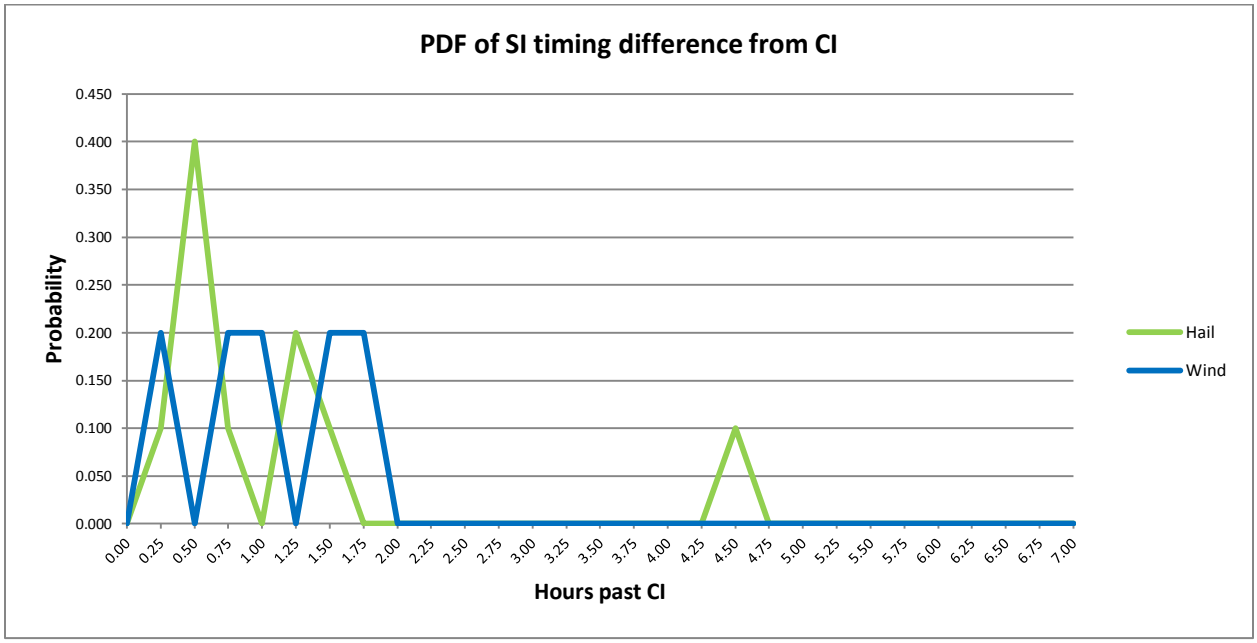

FIG. 4. PDF depicting the time between observed CI and SI associated with convection for each case in the sample.

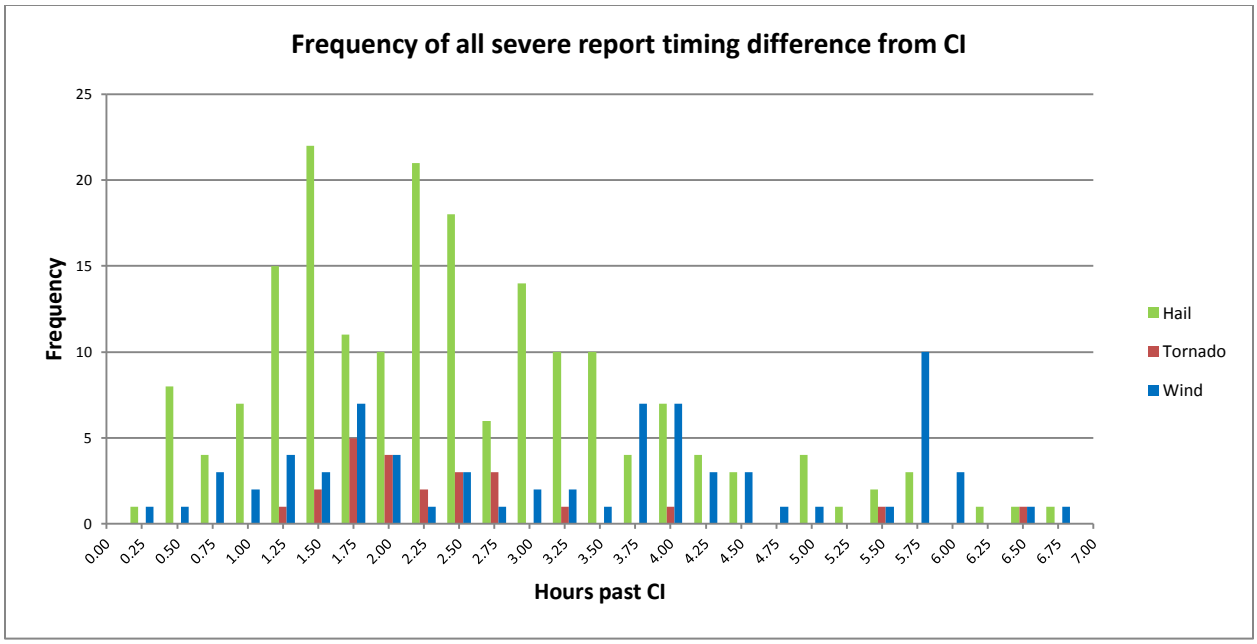

FIG. 5. As in Fig. 3., except for all LSR's associated with convection in the sample.

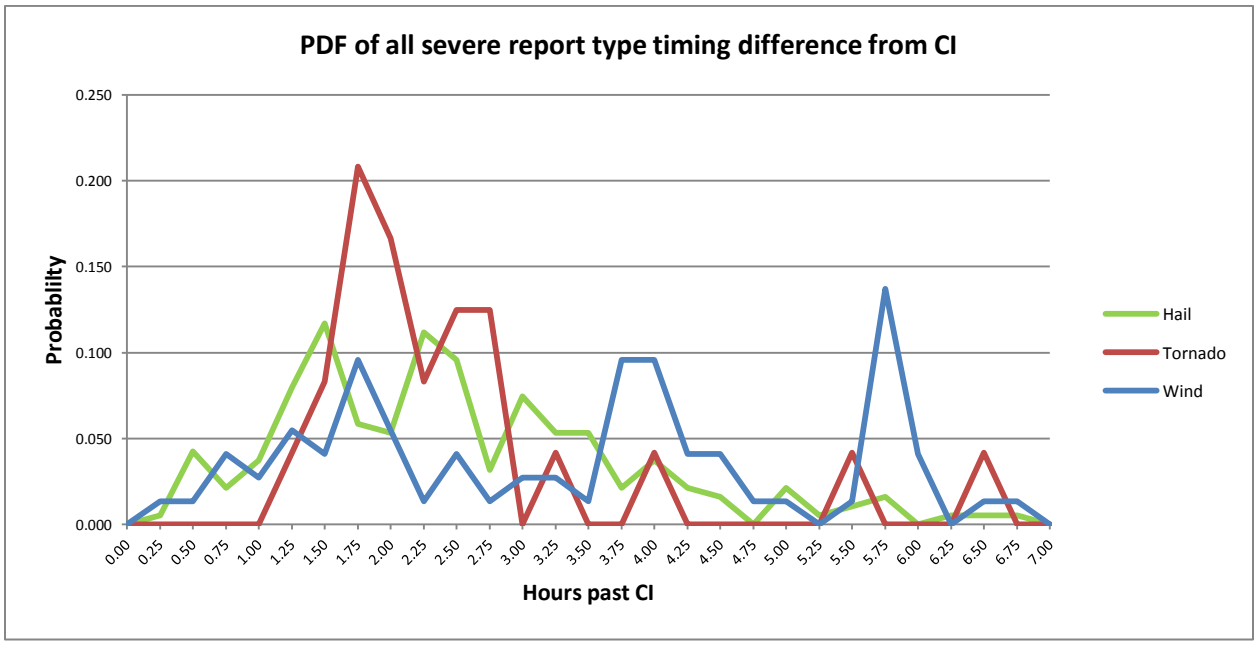

FIG. 6. As in Fig. 4., except for all LSR's associated with convection in the sample.